The mechanism of anodic oxidation of iron-based alloys in molten hydroxides

Tzvety Tzvetkoff

September 24 - 28, 2006 • Maastricht • The Netherlands

Outline

- **Introduction**
- **Aim of the work**
- **Experimental**
- **Results – ac impedance response**
- **Results – ex-situ analysis**
- **Discussion – kinetic model**
- **Discussion – comparison with experiment**
- **Conclusions**

Introduction

- Molten hydroxides are used in descaling baths for ferrous alloys
- Data on the anodic film composition and growth kinetics on these materials in molten hydroxides are very scarce
- No electrochemical studies of the corrosion of steel in molten hydroxide have been reported

Aim of the work

- To characterise the anodic film on Fe-18%Cr in molten NaOH at different temperatures using electrochemical impedance spectroscopy complemented with surface analytical data
- To propose a kinetic model of the passive film on ferritic steel and to estimate some of its parameters

Experimental

- Working electrode material – ferritic steel (17.8%Cr, 0.5%Ni, 0.09%C, 0.8%Si, 0.7%Mn, balance Fe)
- Electrochemical cell: Ni-crucible counter electrode, Mo-reference electrode (E=+0.8 V vs. normal sodium electrode)
- Electrochemical measurements - current vs. potential curves and impedance spectra at different potentials registered – Autolab PGSTAT 30 + FRA module
- Surface Analysis - X-ray photoelectron Spectroscopy (XPS) - ESCALAB Mk II (VG Scientific)
- Fit and simulation – Maple 8.1 and Microcal Origin 6.0

Results - voltammetry

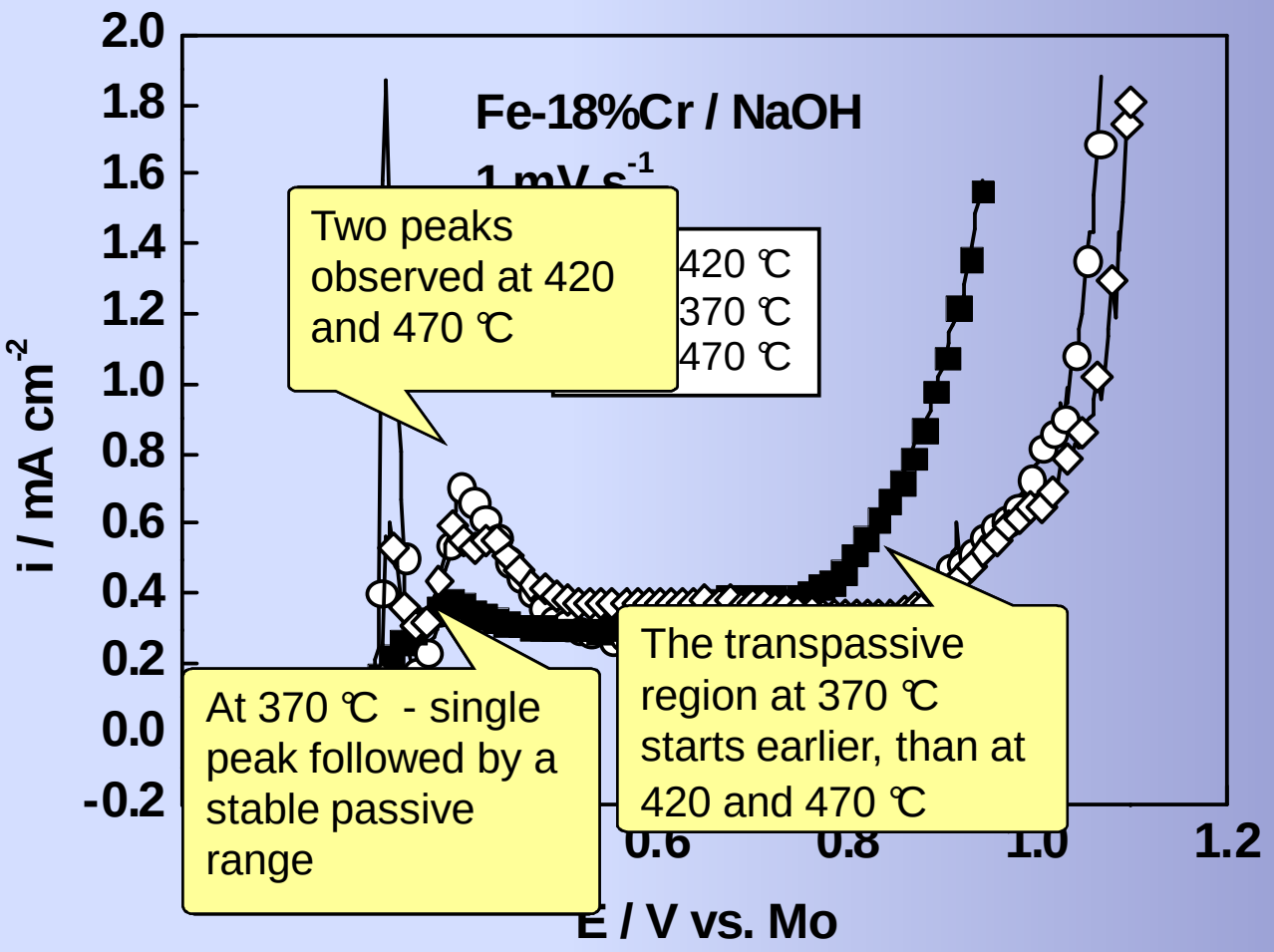

Results – impedance

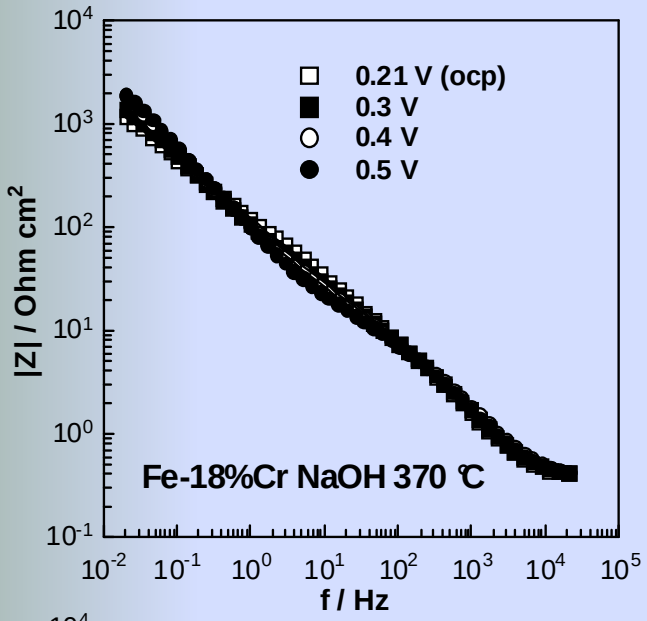

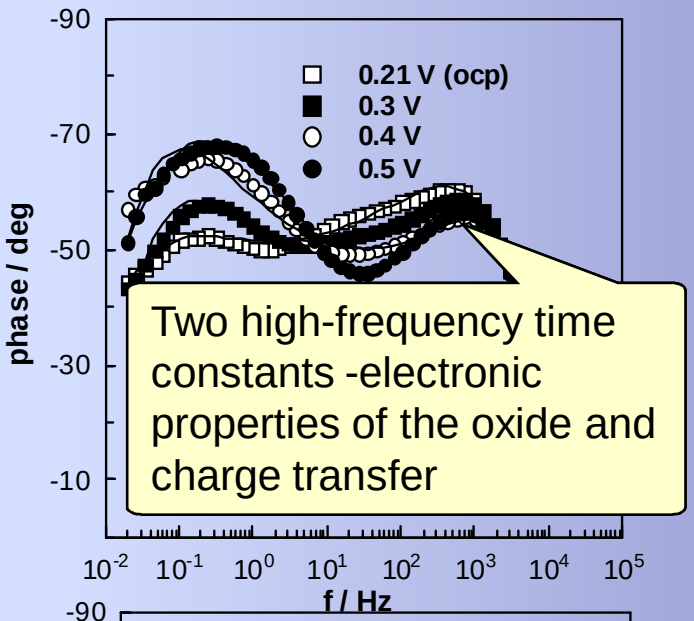

Two high-frequency time constants -electronic properties of the oxide and charge transfer

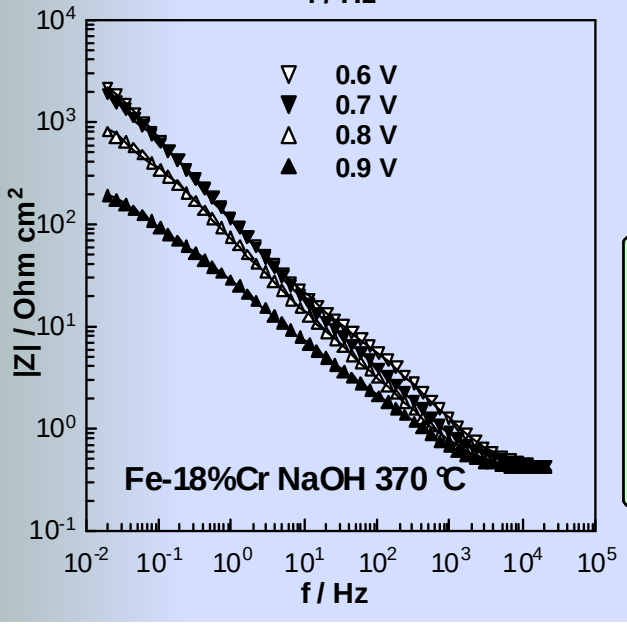

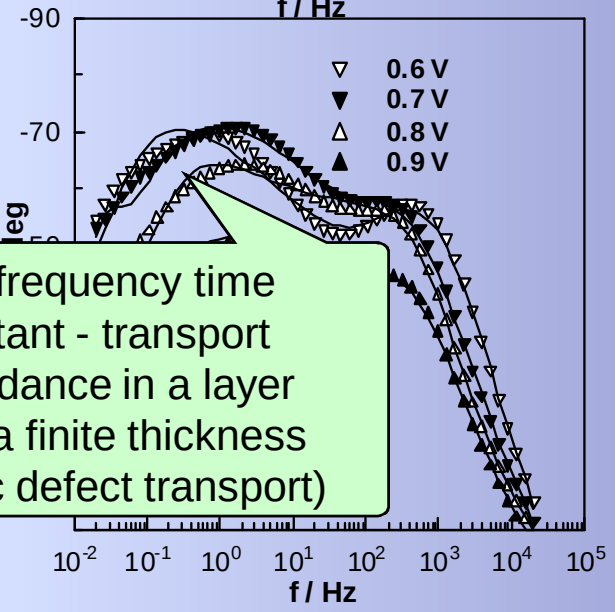

Low-frequency time constant - transport impedance in a layer with a finite thickness (ionic defect transport)

370 °C

Results – impedance (2)

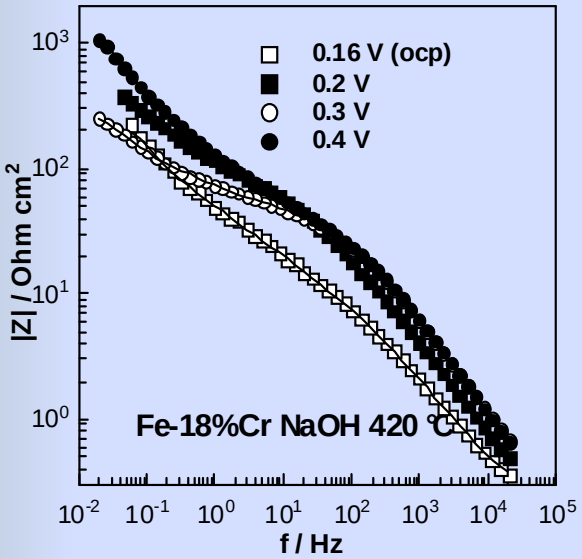

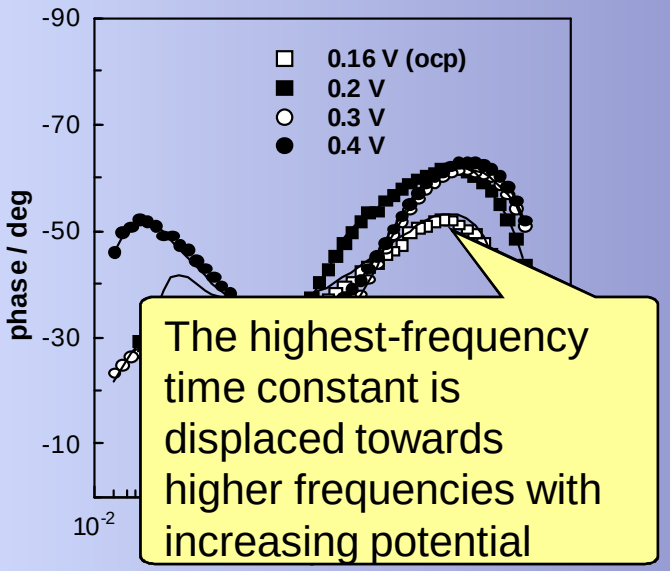

The highest-frequency time constant is displaced towards higher frequencies with increasing potential

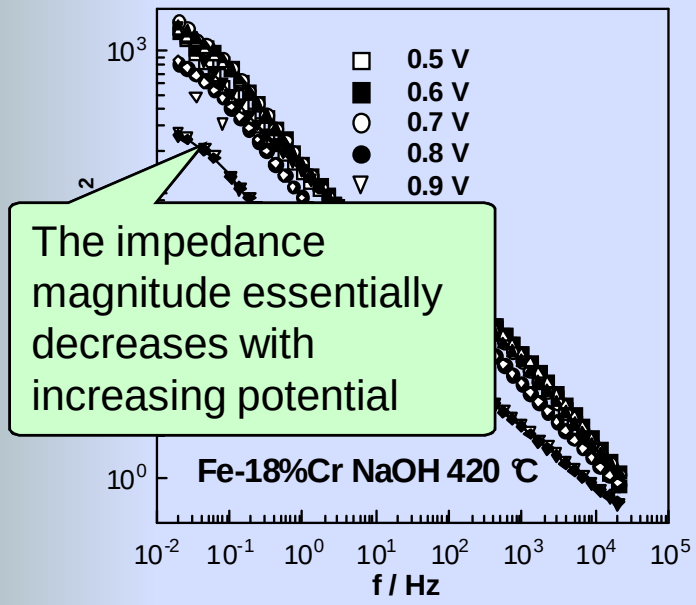

The impedance magnitude essentially decreases with increasing potential

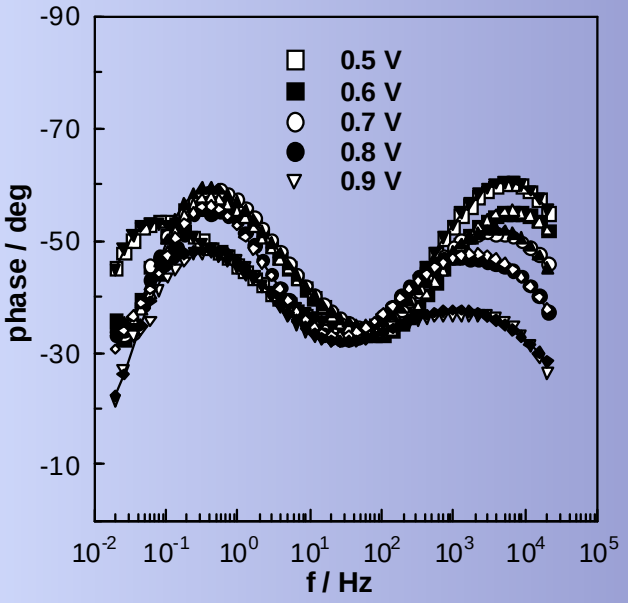

420 °C

Results – impedance (3)

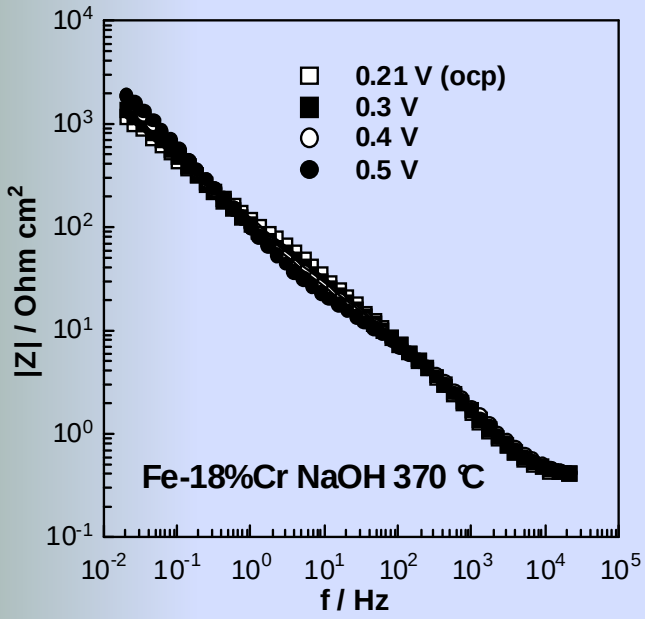

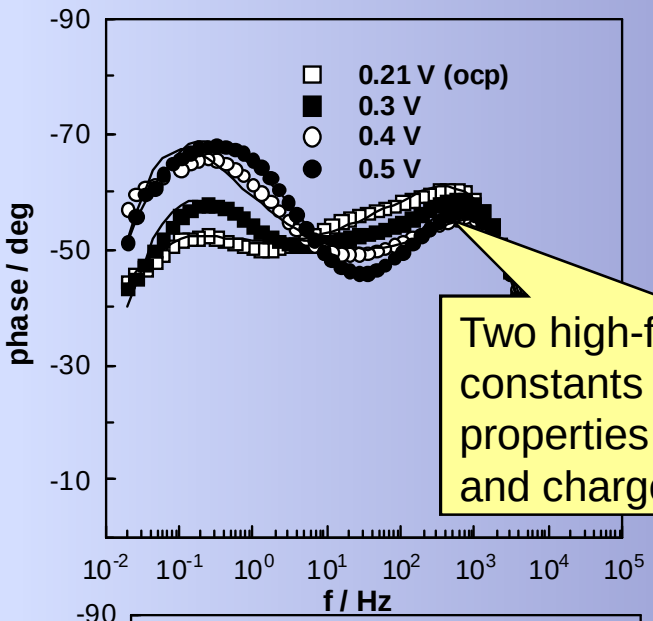

Two high-frequency time constants -electronic properties of the oxide and charge transfer

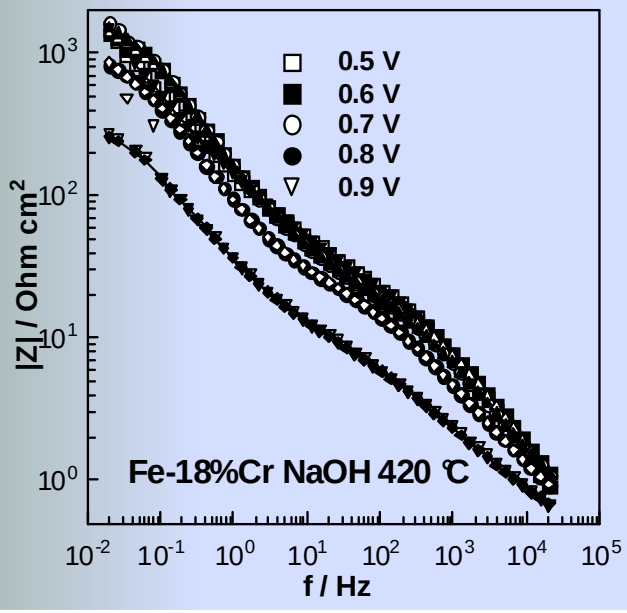

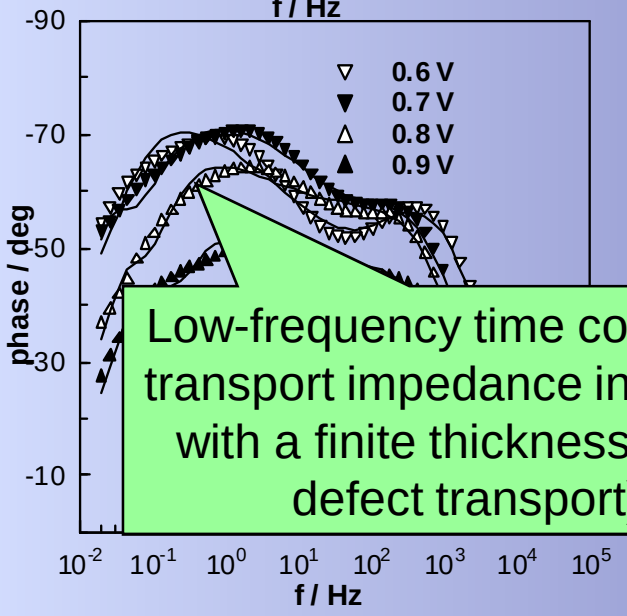

Low-frequency time constant - transport impedance in a layer with a finite thickness (ionic defect transport)

℃

Results – XPS analyses (2)

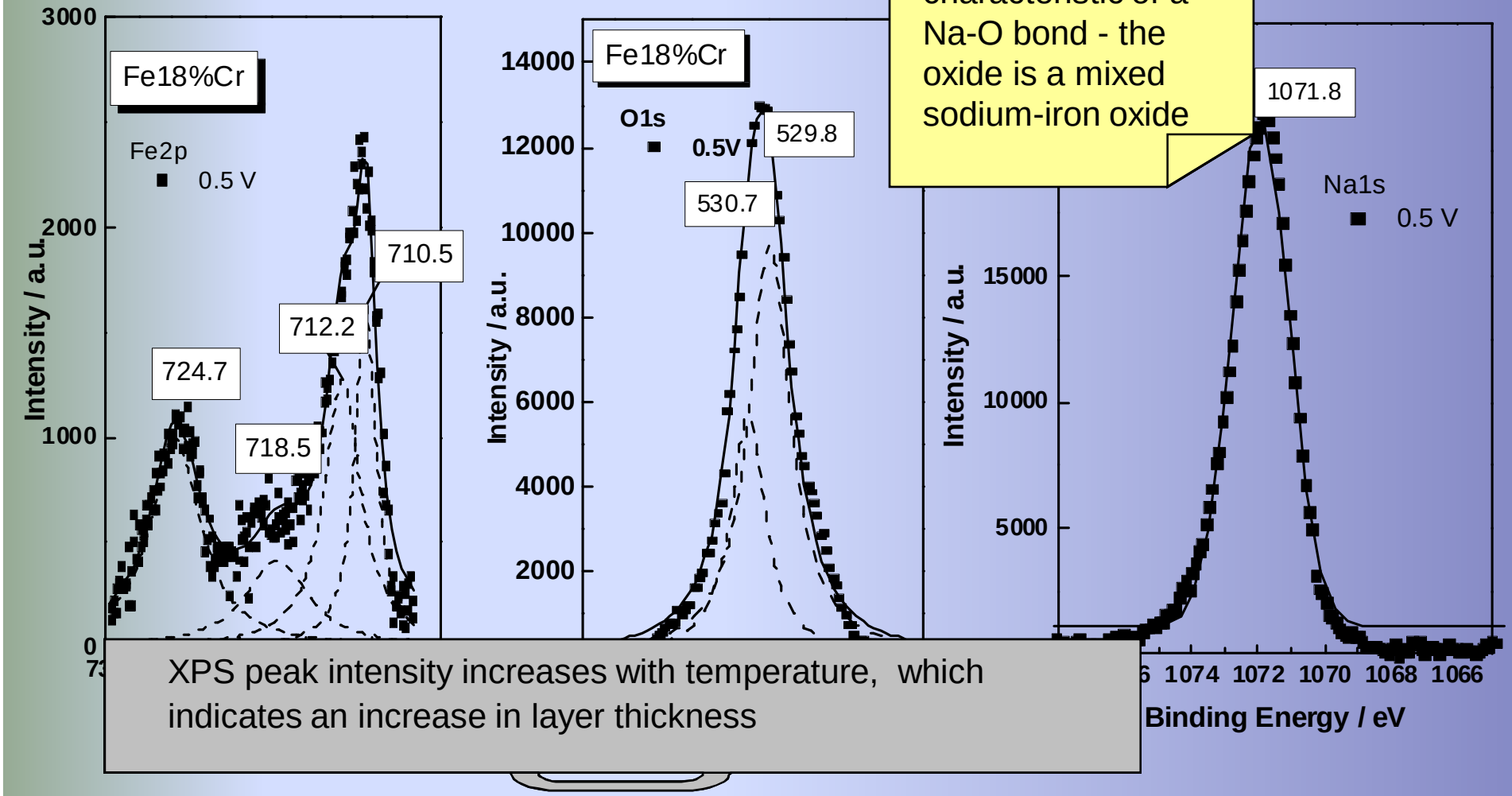

Na1s peak characteristic of a Na-O bond - the oxide is a mixed sodium-iron oxide

XPS peak intensity increases with temperature, which indicates an increase in layer thickness

470 °C

Mixed Conduction Model (MCM)

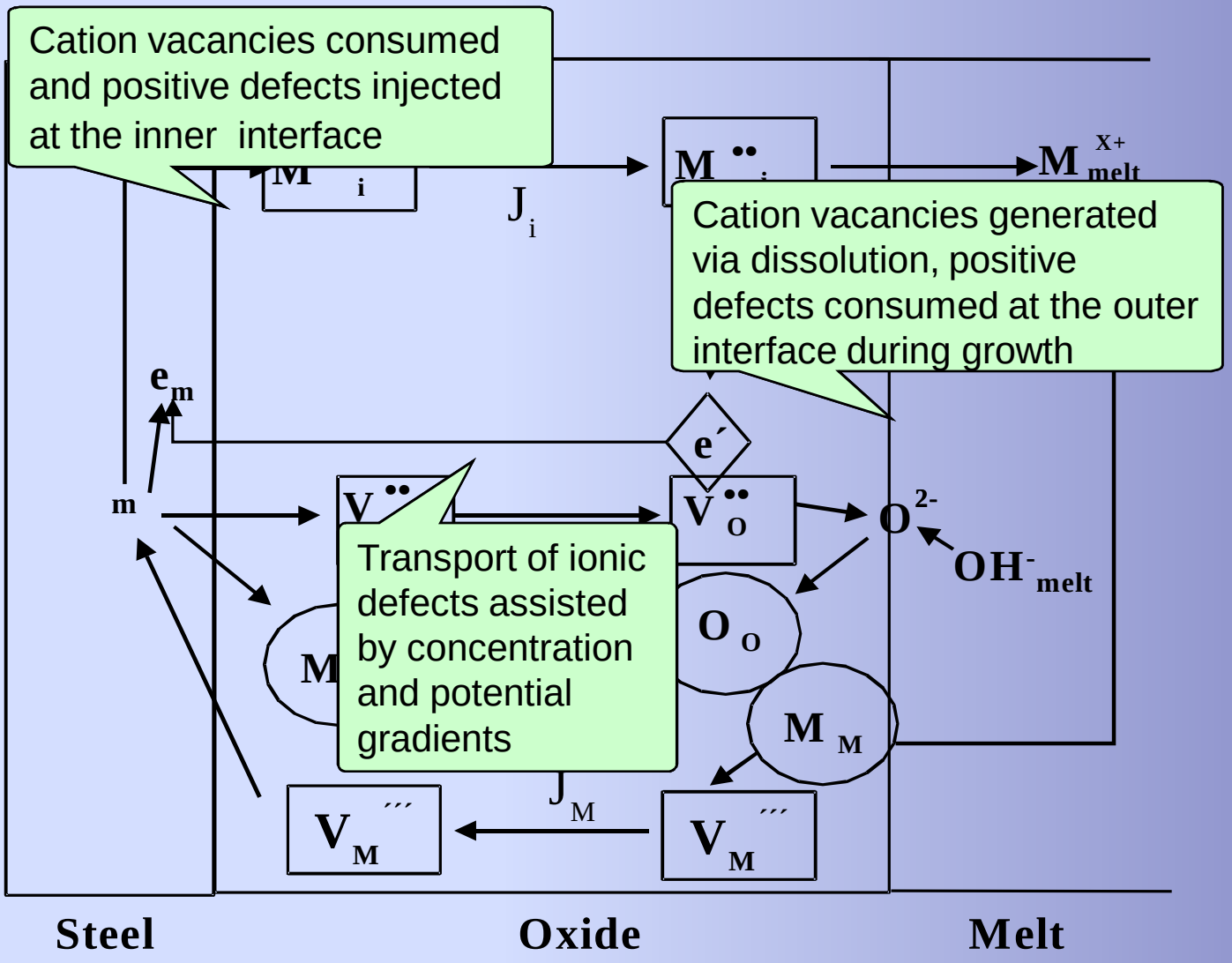

Main equations

Transfer function of the MCM

$$Z = R_{ohm} + \left(\frac{1}{Z_e} + \frac{1}{Z_i} \right)^{-1} + \left(j\omega C_{F/S} + \frac{1}{R_{F/S}} \right)^{-1}$$

Impedance due to the electronic properties of the film

$$Z_e = \frac{p}{j\omega C_{sc}} \ln \left[\frac{1 + j\omega\tau_e e^{\frac{1}{p}}}{1 + j\omega\tau_e} \right] \longrightarrow$$

CPE for $p^{-1} >> \omega\tau_e$

Impedance due to the ionic transport through the film

$$Z_i = R_i + \sigma_i \frac{\tanh\sqrt{j\omega\tau_i}}{\sqrt{j\omega}}$$

$C_{F/S}$ - interfacial capacitance, $R_{F/S}$ - charge transfer resistance
C_{sc} - space charge layer capacitance, σ_I - *Warburg* constant

$$Z = R_{ohm} + \left(\frac{1}{Z_e} + \frac{1}{Z_i} \right)^{-1} + \left(j\omega C_{F/S} + \frac{1}{R_{F/S}} \right)^{-1}$$

- R_{ohm} - uncompensated resistance of the melt,
- $C_{F/S}$ - double layer capacitance at the film / melt interface,
- $R_{F/S}$ - charge transfer resistance of the reaction of secondary layer deposition at the film / melt interface,

- Z_e - electronic contribution to the impedance of the passive film ,
- Z_i - ionic contribution,

- The function Z_e can be regarded as the non-ideal capacitance of a semiconductor layer,
- Z_i accounts for the faradaic impedance of generation, transport and consumption of ionic point defects.

Comparison with experiment

- The transfer function fitted to the experimental spectra at each potential with C_{sc}, $C_{F/S}$, $R_{F/S}$, σ_i and τ_i as free parameters.

- The good correspondence between the calculated and experimental spectra demonstrates the ability of the model to account for the present experimental data.

- Next, the dependencies of the parameters C_{sc}, $C_{F/S}$, $R_{F/S}$, σ_i and τ_i on potential and temperature are compared with the model predictions.

Comparison with experiment (2)

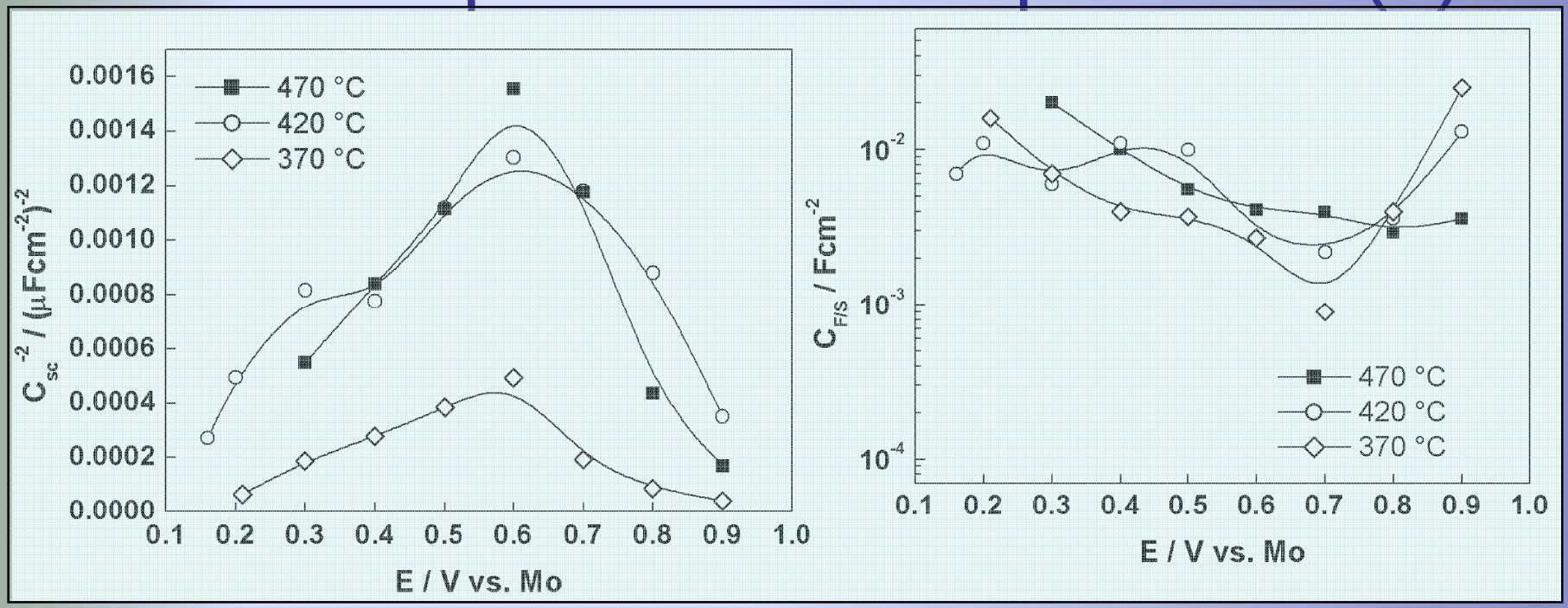

$$C_{sc}^{-2} = \frac{2}{e\varepsilon\varepsilon_0 N_D}\left(E - E_{fb} - \frac{kT}{e}\right)$$

space charge layer capacitance values decrease with increasing temperature

$C_{F/S}$ exhibits relatively large values - reaction pseudocapacitance

capacitance of the film/electrolyte interface is not significantly influenced by temperature

Comparison with experiment (3)

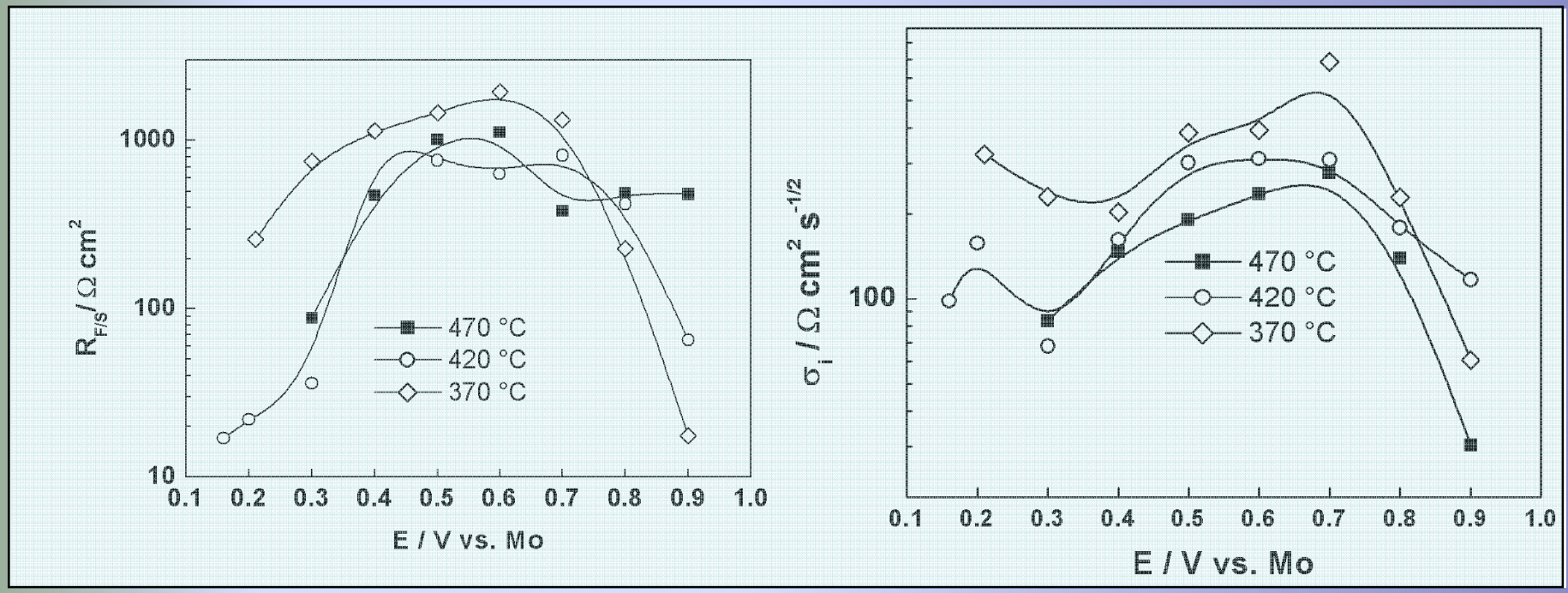

$R_{F/S}$, increases significantly with increasing potential - decrease of the active area available for the interfacial reaction

σ_i decreases with increasing temperature

$$\sigma_i = \frac{RT}{F^2 c_i(L)(1-\alpha)\sqrt{32D_i}}$$

$$c_i(L) = \frac{k_g}{k_c} e^{-2KL} + \frac{k_g}{2KD_i}$$

$$k_c = k_c^0 e^{\frac{2\alpha_c F}{RT}\alpha E}, KL = \frac{F}{RT}(1-\alpha)E$$

Comparison with experiment (4)

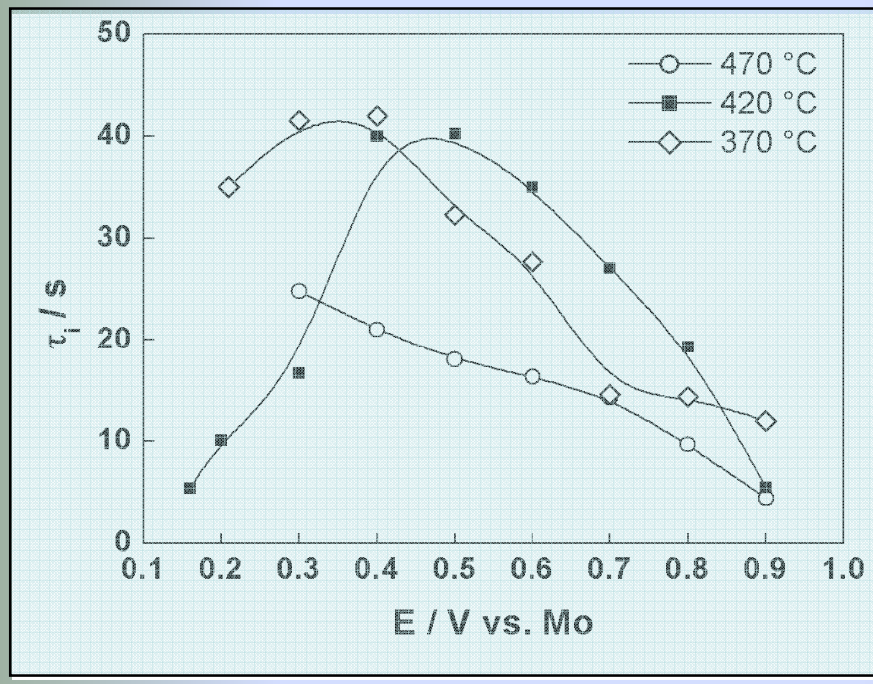

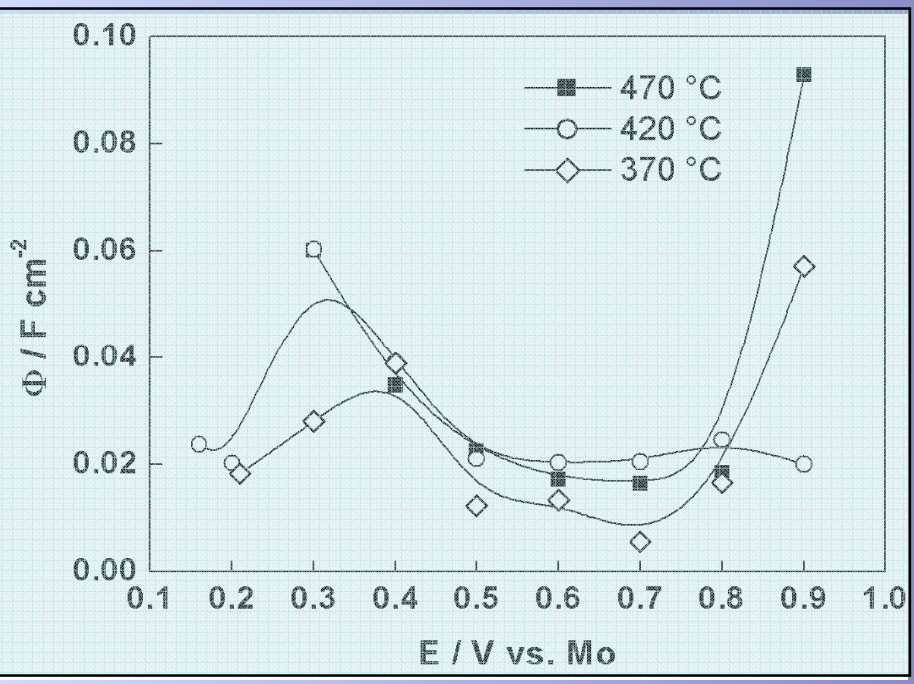

$$\tau_i = \frac{1}{2K^2 D_i}, D_i = D_i(E)?$$

increase of the D_i with temperature
is corroborated by the dependence
of the time constant of the transport process

$$\Phi(E) = \frac{\tau_i^{0.5}}{\sigma_i} = \frac{4Fc_i(L)(1-\alpha)}{E}$$

$$c_i(L) = \frac{k_g}{k_c} e^{-2KL} + \frac{k_g}{2KD_i}$$

$$k_c = k_c^0 e^{\frac{2\alpha_c F}{RT}\alpha E}, KL = \frac{F}{RT}(1-\alpha)E$$

function Φ is an indication that the concentration of current carriers does not depend on temper.

$$Ze \approx [p / j\omega C_{sc}] \ln [(1 + j\omega\tau_e \exp (1 / p)) / (1 + j\omega\tau_e)]$$

- C_{sc}- *capacitance of the space charge layer*,
- L - barrier layer thickness,
- ***E*** - *field strength in the barrier layer,*
- D_e - diffusivity of electronic,
- D_i - *diffusivity of ionic defects,*
- R_∞- resistance of ionic defect migration,
- $c_i(L)$ - *concentration of ionic defects at the metal / film interface*,
- α - polarisability of the film / solution interface,
- k_{1i} - *rate constant of generation of interstitial cations*,
- k_{3i} - rate constant of their consumption at the oxide/melt interface,
- τ_e - *time constant transport process,*

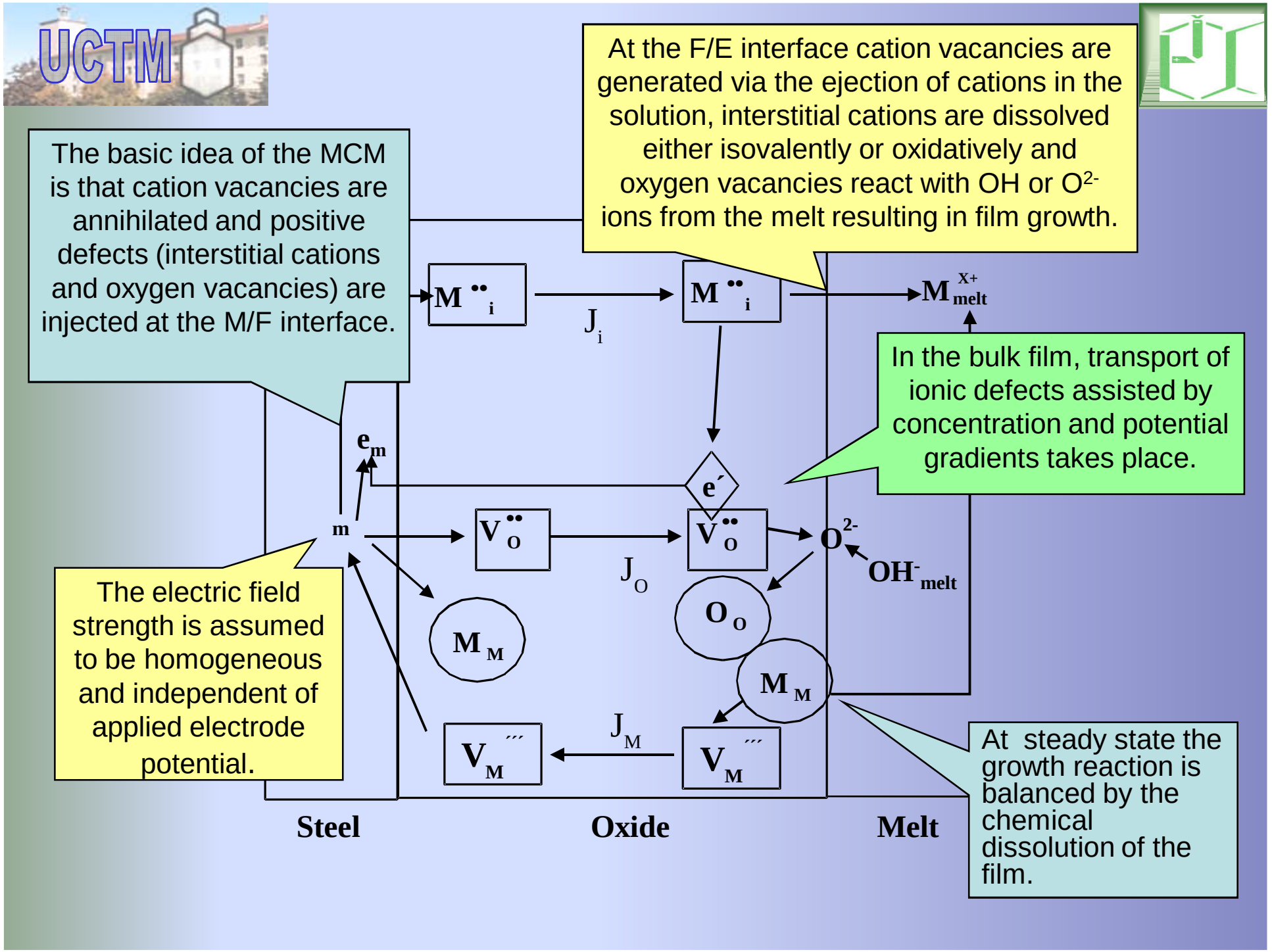
UCTM
At the F/E interface cation vacancies are generated via the ejection of cations in the solution, interstitial cations are dissolved either isovalently or oxidatively and oxygen vacancies react with OH or O^{2-} ions from the melt resulting in film growth.
The basic idea of the MCM is that cation vacancies are annihilated and positive defects (interstitial cations and oxygen vacancies) are injected at the M/F interface.
$M^{\bullet\bullet}_i$
J_i
$M^{\bullet\bullet}_i$
M^{X+}_{melt}
In the bulk film, transport of ionic defects assisted by concentration and potential gradients takes place.
e_m
e'
m
$V^{\bullet\bullet}_O$
J_O
$V^{\bullet\bullet}_O$
O^{2-}
OH^-_{melt}
O_O
M_M
M_M
The electric field strength is assumed to be homogeneous and independent of applied electrode potential.
J_M
V_M'''
V_M'''
At steady state the growth reaction is balanced by the chemical dissolution of the film.
Steel
Oxide
Melt

Conclusions

- The temperature in the range 370-470 ℃ does not h ave a significant influence on the composition, the electrical and electrochemical characteristics of the oxide.
- This fact can be explained by assuming that the processes of oxide growth on ferritic steel in molten hydroxide are controlled by a thin barrier sublayer, the properties of which are not qualitatively altered by temperature.
- This barrier sublayer can be regarded as an intrinsic n-type semiconductor with the principal ionic carriers (iron interstitial cations) playing the role of electron donors.
- Their transport through the oxide and the reaction of precipitation of an outer layer at the barrier sublayer / electrolyte interface can be assumed to be the rate-limiting steps of the overall anodic oxidation process.